Catalysis Today xxx (2016) xxx–xxx

Contents lists available at ScienceDirect

Catalysis Today

journal homepage: www.elsevier.com/locate/cattod

Effect of phosphorus on the activity of Cu/SiO_2 catalysts in the hydrogenolysis of glycerol

C. Sepúlveda[a,*], L. Delgado[a], R. García[a], M. Melendrez[b], J.L.G. Fierro[c], I.T. Ghampson[d], N. Escalona[d,e]

[a] Universidad de Concepción, Facultad de Ciencias Químicas, Edmundo Larenas 129, Casilla 160C, Chile
[b] Universidad de Concepción, Facultad de Ingeniería, Edmundo Larenas 270 exterior, Casilla 160C, Chile
[c] Instituto de Catálisis y Petroleoquímica, CSIC, Cantoblanco, 28049 Madrid, Spain
[d] Departamento de Ingeniería Química y Bioprocesos, Escuela de Ingeniería, Pontificia Universidad Católica de Chile, Avenida Vicuña Mackenna 4860, Macul, Santiago, Chile
[e] Facultad de Química, Pontificia Universidad Católica de Chile, Chile

ARTICLE INFO

Article history:
Received 2 December 2015
Received in revised form 18 April 2016
Accepted 1 June 2016
Available online xxx

Keywords:
Glycerol
Cu
Hydrogenolysis
Octahedral distortion
Electron density

ABSTRACT

The modification effect of P_2O_5 on Cu/SiO_2 catalysts was studied for the hydrogenolysis of glycerol. A series of $Cu/P(y)\text{-}SiO_2$ catalysts with three different loadings of P_2O_5 (2, 3 and 4 wt%) was prepared by successive wet impregnation, and characterized using X-ray Diffraction (XRD), nitrogen sorption, surface acidity technique, UV-Diffuse Reflectance Spectroscopy (UV-DRS) and X-ray Photoelectron Spectroscopy (XPS). The catalysts were evaluated in a batch reactor at 220 °C and 5 MPa of H_2. The addition of phosphorus increased the activity, with the highest activity being achieved over the $Cu(x)/P(y)\text{-}SiO_2$ catalyst with P_2O_5 loading of 2 wt%. The increased activity was attributed to a combination of geometrical and electronic effect induced by P_2O_5 on Cu metallic species. In fact, UV-DRS and TPR measurements showed the existence of a Cu-P interaction, which can increase the distance of the Cu-Cu metal bond, and consequently increase the electron density; this effect enhanced the catalytic activity, compensating for the decrease of Cu dispersion (derived from XPS results). However, this applies only to catalysts with low P_2O_5 loadings because the loss of actives sites by the formation of aggregates at higher P_2O_5 loading cannot be compensated for by Cu-P interaction. The addition of P_2O_5 changes the products distribution because the high electron density of Cu-P favors the adsorption of the C—O bond on glycerol.

1. Introduction

The biofuels industry has become very important in the last decade due to the gradual depletion of crude oil, as well as increased awareness of the negative environmental impact of crude oil. In this context, biodiesel produced from transesterification of vegetables oils has gained a lot of attention because it can be directly used as biofuels, and its usage can reduce greenhouse gas (GHG) emissions in comparison to conventional fuels. However, the transesterification process also produces high quantities of glycerol as a by-product (around 10% in mass) [1] which has contributed to a sharp decline in the price of this compound; furthermore, the large quantity of glycerol represents an environmental risk [2]. Thus, it is critical to find ways to utilize the glycerol produced.

Several researchers have made great efforts to find new applications of glycerol as a low-cost feedstock for functional derivatives [3]. For example, a series of selective processes for converting glycerol into products with high-added value have been proposed, including selective oxidation, etherification, hydrogenolysis, dehydration, fermentation, refined glycerol, among others [1,4–7].

Selective hydrogenolysis of glycerol in the presence of hydrogen and bifunctional catalysts can produce 1.2-propanediol (1.2-PDO), 1.3-propanediol (1.3-PDO) or ethylene glycol (EG) as main products [8–10]. 1,2 PDO is used principally in the chemical industry to produce polyester resins, liquid detergents, pharmaceuticals, cosmetics, flavours and fragrances, personal care, paint, pet food, antifreeze, among others [1]. On the other hand, 1.3-PDO is commonly used for the production of polyesters and polyurethane resins [11,12].

* Corresponding author.
E-mail addresses: cathsepulveda@udec.cl, catherinesepulvedamunoz@gmail.com (C. Sepúlveda).

http://dx.doi.org/10.1016/j.cattod.2016.06.004
0920-5861/

Among the choices of heterogeneous catalysts for the selective hydrogenolysis of glycerol, copper has been found to be highly active because it is a good hydrogenating catalyst [13,14], it exhibits low activity towards breaking C—C bonds, and it is highly efficient in C—O bonds hydrogenation and dehydrogenation. Copper catalysts have been reported to be highly selective towards propanediols, especially1.2-PDO [8,10,15]. Vila et al. [16] proposed that glycerol conversion is favored by an optimal Cu^0/Cu^+ atomic ratio, while the selectivity towards 1.2-PDO formation was attributed to the principal presence of Cu^0.

In relation to supports, acidic supports with diverse textural properties such as SiO_2-Al_2O_3, zeolites, Al_2O_3, ZrO_2, activated carbons, etc. have been used to prepare Cu catalysts for the hydrogenolysis of glycerol because of the critical functions of the acidic and textural properties of the supports on this reaction [16–20]. However, SiO_2 can also be an effective support for glycerol hydrogenolysis: its activity and selectivity has been reported to depend on the interplay between the impregnation method and the high metal specific surface area of the active component [8,21].

As previously mentioned, the acidity of the catalysts is fundamental in this type of reaction. Phosphorous has been used to modify the acidic nature of catalysts to change the activity and selectivity in hydrotreating reactions [22–24]. In hydrodesulfurization (HDS) reactions, the addition of P to NiMo/Al_2O_3 catalysts led to an optimal combination of acidity and porosity which improved the dispersion of the active phase on the support, enhancing the activity and stability of the catalysts [22]. Along the same line, Leiva et al. [23] studied the effect of the addition of P on Mo/γ-Al_2O_3 catalysts in hydrodeoxygenation (HDO) reaction, specifically, the conversion of guaiacol. The authors found that the addition of P modified the activity which reached a maximum activity at 1.0 wt% P. This change was correlated with MoS_2 dispersion. Also, the products selectivity was modified, attributed to changes in acid strength by P addition. Huang *et. al* [24]. compared the activity and selectivity of Ni_2P/SiO_2 and Ni/SiO_2 catalysts in hydrogenolysis of glycerol and found that P improves the catalytic activity attributed to synergism of acid and metallic sites from P-OH and Ni, respectively. The authors proposed that P addition favours C—O bond cleavage over C—C bond scission observed with Ni/SiO_2 catalyst, and attributed this behaviour principally to geometric and electronic properties.

On the other hand, the effect of phosphorus on Cu catalysts supported on SiO_2 has not been studied. Therefore, the objective of this work was to study the P effect on the activity and products distribution of Cu/P(y)-SiO_2 catalysts in glycerol conversion. The catalysts were characterized by different techniques in order to correlate their activities with the structure of the solids.

2. Experimental

2.1. Catalyst preparation

The Cu/SiO_2 and Cu/P(y)-SiO_2 catalysts were prepared by successive impregnation steps. Prior to the metal impregnation, the SiO_2 (Grace 432, Davidson) support was ground and sieved to obtain particle sizes between 80 and 125 μm. Then, the support was impregnated with an aqueous solution of H_3PO_4 to obtain final catalysts with three P loadings (2, 3 and 4 wt.% calculated on P_2O_5 basis). The range of phosphorous loading was selected according to previous research, because P loading above 2 wt% increases the acid strength of the catalysts [23]. Phosphoric acid (85 m/v%) was also added to SiO_2 in addition to 10 mL of deionized water. The pH was adjusted between 1.5 and 2.0 with HNO_3 (65 m/v%). Then, the mixture was homogenized in a rotary evaporator for 3 h at room temperature. The excess solvent was removed under vacuum at 55 °C. Finally, the modified support (P (y)-SiO_2) was dried for 12 h at 120 °C and calcined at 550 °C for 4.5 h under static air [23].

The Cu/SiO_2 and Cu/P(y)-SiO_2 catalysts were prepared by wet impregnation of aqueous copper (II) nitrate ($Cu(NO_3)_2{\cdot}3H_2O$, Aldrich) to obtain a 20 wt% of Cu. The mixture was first homogenized for 4 h at 55 °C in a rotary evaporator; then, the excess solvent was removed under vacuum at 55 °C. Finally, the samples were dried at 120 °C for 12 h and calcined at 500 °C for 2 h under static air. Before the reaction, the catalysts were reduced *ex-situ* at 400 °C for 4 h in flowing H_2 (60 mL min^{-1}). The Cu and P contents were determined by atomic absorption spectroscopy using a Thermo Scientific ICE 3000 model series.

2.2. Characterization of supports and catalysts

The BET specific surface area (S_{BET}) and pore volume of the supports and catalysts were determined from nitrogen sorption measurements at −196 °C using Micromeritics TriStar II 3020 equipment. Prior to the measurements, the samples were degassed at 300 °C for 2 h. Micropore volume (Vo) was determined by the Dubinin–Radushkevich method while the total pore volume (Vp) was recorded by nitrogen adsorption at a relative pressure of 0.99. Mesopore volume (Vm) was determined by the difference between Vp and Vo.

Temperature programmed reduction (TPR) was carried out in a quartz cell in a system equipped with a thermal conductivity detector. In the experiment, 20 mg of the sample was heated under 5% H_2/Ar flowing at 50 mL min^{-1}. The sample was heated at 10 °C min^{-1} from 25 °C to 1050 °C.

Powder X-ray Diffraction (XRD) were obtained using a D4 Endeavor Bruker AXS diffractometer equipped with a nickel-filtered CuKα_1 radiation (λ= 1.5418 Å). The standard scan parameters were 1° per min for the 2θ range from 10 to 90°. Identification of the phases was achieved by reference to ICDD files.

The Diffuse Reflectance UV–vis measurements were carried out using a Lambda 35 spectrophotometer. The Kubelka- Munk's equation was used to calculate the intensities (I_{OH}/I_{OHd}) ratio between Cu^{2+} octahedral species (I_{OH}) and octahedral distorted Cu^{2+} species (I_{OHd}) as a function of P_2O_5 content.

The total acidity of the support and the reduced catalysts were measured potentiometrically by suspending the catalysts in acetonitrile and titrating with *n*-butylamine using an Ag/AgCl electrode [25].

The XPS measurements were performed using a VG Escalab 200 R electron spectrometer equipped with a hemispherical electron analyzer and Mg Kα (1253.6 eV) X-ray source. The samples were reduced *in-situ* at 673 K under H_2 flowing and transferred from the pretreatment chamber to the spectrometer. The intensity of the peaks was estimated by calculating the integral of each peak after subtracting an S-shaped background and fitting the experimental curve to a combination of Gaussian/Lorentzian lines. Atomic ratios were calculated by using peak areas normalized on the basis of acquisition parameters, sensitivity and transmission factors provided by the manufacturer, and determined from the corresponding peak intensities, corrected with tabulated sensitivity factors, with a precision of ±7%.

2.3. Catalytic reaction test

Hydrogenolysis of glycerol was performed in a 300 mL batch reactor 4848 Parr model. The concentration of glycerol used was 10 mol L^{-1}. This concentration was selected after rigorous study of the optimal glycerol amount to avoid the high vapor pressure of water and the burning of glycerol. Also, the mass of the catalyst used was selected from experimental study of mass of solid necessary to keep the reaction in kinetic regime. In this context,

Please cite this article in press as: C. Sepúlveda, et al., Effect of phosphorus on the activity of Cu/SiO_2 catalysts in the hydrogenolysis of glycerol, Catal. Today (2016), http://dx.doi.org/10.1016/j.cattod.2016.06.004

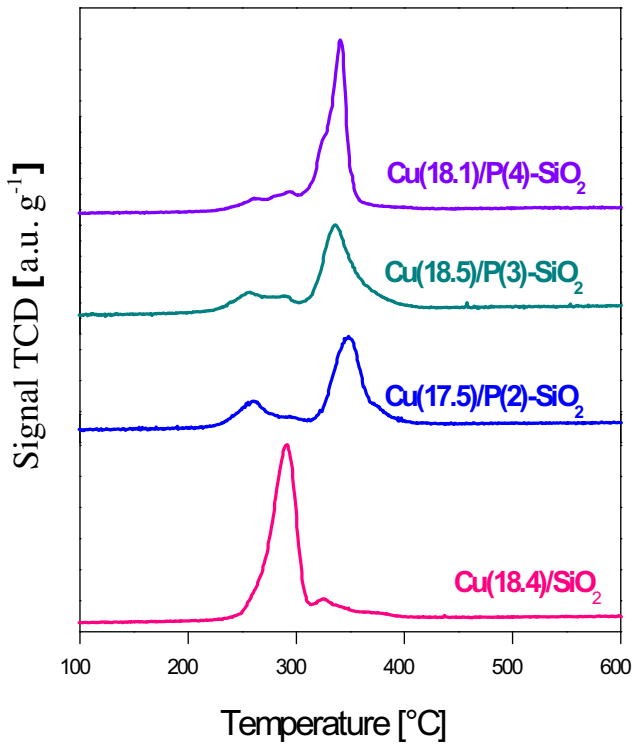

Fig. 1. Temperature-programmed reduction (TPR) of calcined Cu(x)/SiO_2 and Cu(x)/P(y)-SiO_2 catalysts.

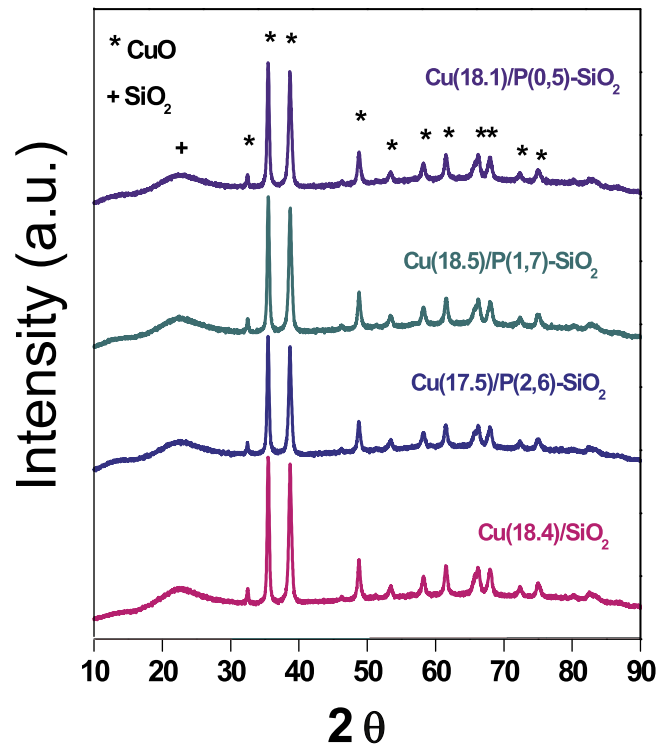

Fig. 2. X-ray diffraction patterns of calcined Cu(x)/SiO_2 and Cu(x)/P(y)-SiO_2 catalysts.

the liquid reactant feed consisted of an aqueous glycerol solution (80 wt.%). About 0.5 g of pre-reduced catalyst was added to the reactant. Then, the system was closed and N_2 was bubbled through the solution for 10 min to avoid any air contamination. Still under N_2, the reactor was heated to the reaction temperature of 220 °C while stirring. When the reaction temperature was reached, H_2 was introduced into the reactor to 5 MPa which was kept constant during the course of the experiment. Condensed samples were taken periodically during the reaction and were identified and quantified using a Perkin Elmer Autosystem XL gas chromatograph with a flame ionization detector equipped with a column (Nukol, 30 m x 0.53 mm x0.5 μm). The catalytic activity was calculated after 22 h of reaction according to Eq. (1):

$$r = \frac{m}{g_{cat} \times s} \quad (1)$$

where m is mol of glycerol converted after 22 h calculated from initial mol of reactant introduced in the reactor, g_{cat} is the mass of the catalyst (grams), and s is the total time of reaction expressed in second. The products distribution was calculated when the reaction was completed.

3. Results and discussion

3.1. Catalysts and support characterization

The textural properties of the SiO_2 and P(y)-SiO_2 supports, Cu(18.5)/SiO_2 and Cu(x)/P(y)-SiO_2 catalysts are presented in Table 1. The addition of P to SiO_2 support slightly modified the textural properties: the observed changes in surface area can be attributed to the 10% error associated with these measurements. Upon Cu impregnation, the textural properties decreased which can be attributed to pore blockage by Cu species.

Fig. 1 shows the TPR profiles of calcined Cu(x)/SiO_2 and Cu(x)/P(y)-SiO_2 catalysts. In this figure, two reduction peaks can be seen in all the catalysts. The Cu(18.4)/SiO_2 catalyst displayed a main peak at around 300 °C, while a low-intense shoulder can also be observed around 340 °C. The peak at 300 °C can be attributed to the reduction of highly dispersed CuO species from Cu^{2+} to Cu^0 [26,27], while the shoulder at 340 °C can be attributed to the reduction Cu^+ to Cu^0 [28,29], suggesting that this is an intermediate species in the reduction step. In contrast, the Cu(x)/P(y)-SiO_2 catalysts presented less intense peaks at 300 °C attributed to the reduction of highly dispersed CuO [26,27], while the principal peak observed at 350 °C was assigned to the reduction of Cu^{2+}-like O—Cu-P interaction [30]. Finally, the formation of phosphates or Cu polyphosphates was not detected from TPR analyses. The H_2 consumption was calculated after calibration by the reduction of a reference CuO solid: the Cu(x)/SiO_2 and Cu(x)/P(y)-SiO_2 catalysts presented Cu reducibility of 95% and 98%, respectively, indicating almost complete reduction of Cu species.

Fig. 2 presents the XRD results of calcined un-modified and modified catalysts. All the catalysts showed diffraction peaks at 2θ = 31°, 35°, 38°, 48°, 53°, 58°, 61°, 66°, 67°, 72°, 74° and 82°, assigned to CuO [29]. This result suggests that the addition of small amounts of P to the support did not modify the Cu crystalline structure. In addition, phosphates or Cu polyphosphates species were not detected, in agreement with TPR results.

The UV-DRS spectra of Cu(18.4)/SiO_2 and Cu(x)/P(y)-SiO_2 catalysts are shown in Fig. 3. The P(2)-SiO_2 support displayed a band between 280 and 400 nm, while the other catalysts displayed two reflectance bands between 250 and 580 and 800–1000 nm. The bands between 280 and 580 nm were associated with octahedral geometry (hexacordinated symmetry) of Cu^{2+} species [31–33]. Meanwhile, the bands around 800–1000 nm were attributed to d-d electronic transition of Cu^{2+} according to distorted octahedral geometry (pentacoordinated symmetry) [31–33]. In order to determine the effect of P_2O_5 on the symmetry of CuO species, the intensities (I_{OH}/I_{OHd}) ratio between Cu^{2+} octahedral species (I_{OH}) and octahedral distorted Cu^{2+} species (I_{OHd}) as a function of P_2O_5 content is shown in Fig. 4. It can be seen that (I_{OH}/I_{OHd})

Table 1
Textural and chemical properties of SiO_2 and P(y)-SiO_2 supports, Cu(x)/SiO_2 and Cu(x)/P(y)-SiO_2 catalysts.

	S_{BET} $[m^2g^{-1}]$	V_p[a] $[cm^3g^{-1}]$	V_o[b] $[cm^3g]$	V_m[c] $[cm^3g]$	Total acidity (mV)
Supports					
SiO_2	320	1.13	0.14	0.98	−2
P(2)-SiO_2	298	1.07	0.14	0.93	399
P(3)-SiO_2	321	1.10	0.15	0.95	–
P(4)-SiO_2	303	1.07	0.14	0.93	322
Catalysts					
Cu(18.4)/SiO_2	238	0.84	0.11	0.73	−50.8
Cu(17.5)/P(2)- SiO_2	229	0.79	0.11	0.69	−66.3
Cu(18.5)/P(3)- SiO_2	239	0.83	0.11	0.72	−72.3
Cu(18.1)/P(4)- SiO_2	251	0.87	0.12	0.75	−58.7

[a] V_p: pore volume.
[b] V_o: micropore volume.
[c] V_m: mesopore volume.

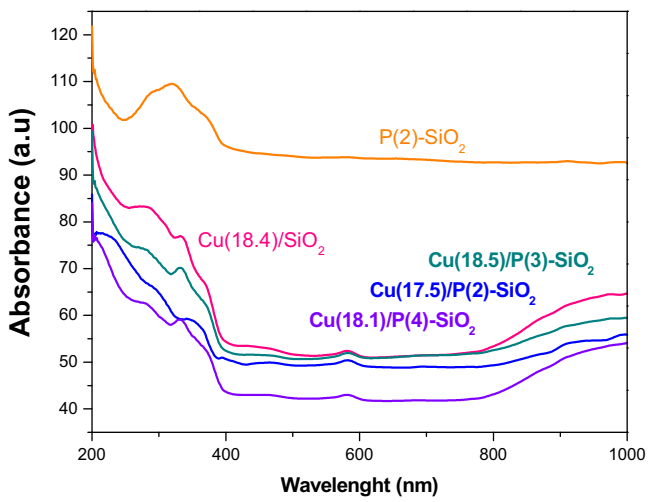

Fig. 3. UV–vis diffuse reflectance spectra (UV-DRS) of calcined Cu(18.4)/SiO_2 and Cu(x)/P(y)-SiO_2 catalysts.

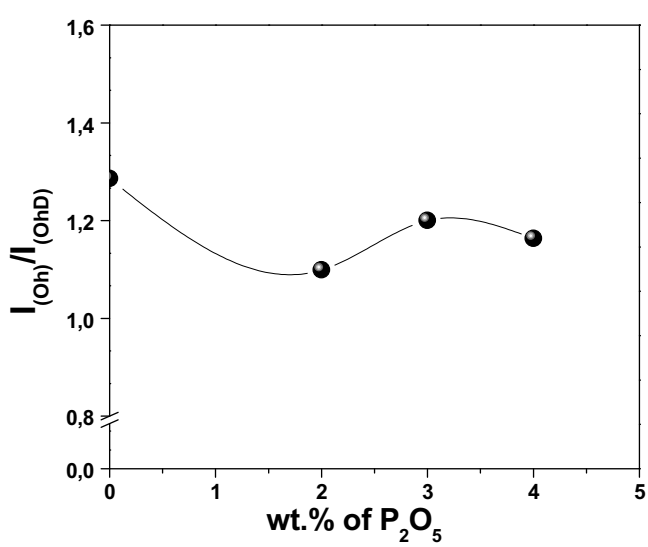

Fig. 4. Intensities (I_{OH}/I_{OHd}) ratio between Cu^{2+} octahedral species (I_{OH}) and octahedral distorted Cu^{2+} species (I_{OHd})n as a function of P_2O_5 content.

ratio decreased after P_2O_5 addition, reaching the minimum value at 2 wt% of P_2O_5, and then increased slightly with P content. These results suggest that the addition of P_2O_5 distorts the characteristic octahedral symmetry of CuO species formed during calcination, probably due to an effect of O-Cu-P interaction, as suggested by

Table 2
XPS binding energies (eV) and surface atomic ratio of Cu(x)/SiO_2 and Cu(x)/P(y)-SiO_2 reduced catalysts.

Catalysts	$Cu2p_{3/2}$ (eV)	P2p (eV)	Cu/Si at	P/Si at
Cu(18.4)/SiO_2	932.7	–	0.218	–
Cu(17.5)/P(2)-SiO_2	932.6	133.7	0.189	0.0020
Cu(18.5)/P(3)-SiO_2	932.7	133.8	0.178	0.0024
Cu(18.1)/P(4)-SiO_2	932.8	133.8	0.172	0.0029

TPR results. The distortion of the octahedral symmetry of Cu by P_2O_5 could increase the distance of the Cu-Cu metallic bonds, similar to that observed for Ni catalysts [34], favouring an increase in the electron density of Cu-P [35]. This effect may increase the catalytic activity of Cu(x)/P(y)-SiO_2 in comparison to Cu(18.4)/SiO_2 catalysts.

The acid strength determined by potentiometric titration and expressed as total acidity (E_0) is summarized in Table 1. All the solids were reduced prior to the measurements. The acid strength can be determined according to the criterion proposed by Cid and Pecchi [25]: $E_0 > 100$ mV, very strong acid sites; $0 < E_0 < 100$ mV, strong acid sites; $-100 < E_0 < 0$ mV, weak acid sites; $E_0 < -100$ mV, very weak acid sites. The results indicate that the addition of P increased the acidity of the SiO_2 support to very strong acid sites. The results suggest that acid strength depends on the nature of P-SiO_2 interaction. Fitz et al. [36] proposed that one hydroxide group bonded to tetrahedral Al ions on the surface of Al_2O_3 supports can react with one of the four hydroxide groups of H_3PO_4 (aq) to form a O—O bond. The authors suggested that there will be an increase in the surface acidity of the solid if the phosphoric acid molecule binds to alumina, due to the presence of two available acidic H_2 from the phosphoric acid. Therefore, the observed increase of acidity after P addition can be attributed to P-Si interaction by one OH-group of SiO_2 formed in the aqueous phase and one OH-group of phosphoric acid during impregnation. Notably, the Cu/SiO_2 and all the Cu/P(y)-SiO_2 catalysts presented weak acid sites after impregnation of copper: this behaviour can be attributed to the interaction of Cu^{2+} with OH-sites of SiO_2 and P_2O_5-SiO_2 which decreased the overall acidity.

Fig. 5 shows the XP spectra of reduced Cu(18.4)/SiO_2 (5a) and Cu(x)/P(y)-SiO_2 (5b, c and d) catalysts. Fig. 5(a–d) shows only one doublet for the Cu $2p_{3/2}$ peak for all the catalysts, indicating the presence of only one phase. Table 2 summarizes the binding energies (BE) of the most intense Cu $2p_{3/2}$ component of each doublet, the P $2p_{3/2}$ contribution, the Cu/Si, and P/Si surface atomic ratios for all catalysts studied. Table 2 shows that the contribution of binding energies for Cu in all the catalysts is at 932.7 ± 0.1 eV, assigned to Cu^0 species [16,37], indicating that P addition did not modify the nature of the active sites. The binding energy at 133.7 ± 0.1 eV for P $2p_{3/2}$ is assigned to P_2O_5 species [38]. Fig. 6 shows the Cu/Si and P/Si atomic ratios as a function of P_2O_5 wt%: a gradual increase of

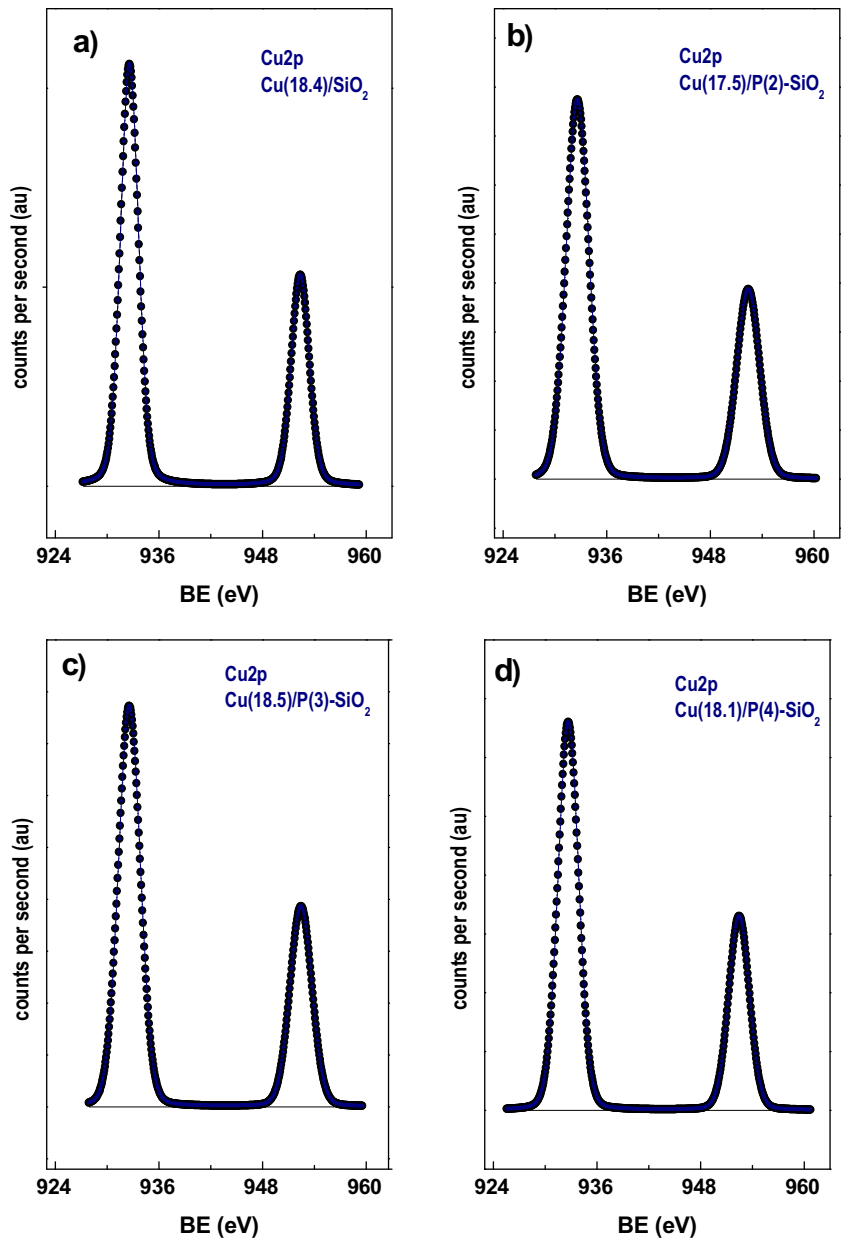

Fig. 5. XP spectra of Cu 2p in reduced a) Cu(18.4)/SiO_2 b) Cu(17.5)/P(2)-SiO_2 and c) Cu(18.5)/P(3)-SiO_2 and d) Cu(18.1)/P(4)-SiO_2 catalysts.

P/Si atomic ratio with P_2O_5 content can be observed, suggesting a homogeneous distribution of phosphorous on the support surface. Conversely, Cu/Si atomic ratio decreased with P_2O_5 loading. This observed trend suggests that Cu-P interaction decreases the homogeneous distribution of Cu on SiO_2, leading to a gradual loss of Cu dispersion. In fact, TPR results show the reduction of CuO species interacting with P_2O_5, while UV-DRS results (Fig. 4) suggest a distortion of the octahedral geometry of some CuO species because of the interaction of Cu-P (P_2O_5). Taken together, these results are consistent with the total acidity measurements, where an observed increase in acid strength after P addition was attributed to P-SiO_2 interaction.

3.2. Catalytic activity of Cu(x)/SiO_2 and Cu(x)/P(y)-SiO_2 catalysts

The transformation pathway in the hydrogenolysis of glycerol include two principal routes: (i) C—C bond breaking, were glycerol can convert to ethyleneglycol and methanol by hydrogenation; (ii) dehydration of glycerol via C—O bond cleavage, forming hydroxyacetone (acetol) and 3-hydroxipropanal as intermediates, and subsequent hydrogenation to 1.2-PDO and 1.3-PDO [15–17]. 3-hydroxipropanal can be further dehydrated to 2-propenal (acrolein) and propanoic acid [15–17].

Table 3 summarizes the rate of glycerol transformation (mol of glycerol converted per gram of catalyst per second) on all the catalysts studied, and the distribution of the main products (expressed in percentage). This table shows that the activity increases with 2 wt% P loading and then decreases. Huang et al. [24] proposed that the electronic and geometrical properties of catalysts induced by the addition of P may influence the adsorption of glycerol and, thus, influence the selectivity. Along the same line, Lee and Oyama [35] suggested that Ni_2P catalysts has a high electron density which is capable of forming π-back-bonded CO species on Ni sites, and moderate acidity in the form of PO-H form; both of these species

Table 3
Catalytic activity of Cu(x)/SiO_2 and Cu(x)/P(y)-SiO_2 catalysts.

Catalysts	Rate *10^7 (mol g_{cat}^{-1} s^{-1})	Products distribution (%)					
		1.2PDO	1.3PDO	Propanic acid	acrolein	1-propanol	Ethyleneglycol
Cu(18.4)/SiO_2	9.9	23.5	7.9	14.0	8.4	36.8	9.5
Cu(17.5)/P(2)-SiO_2	22.4	2.1	10.2	30.3	19.9	33.4	13.1
Cu(18.5)/P(3)-SiO_2	18.6	5.0	12.7	28.9	15.2	22.9	15.4
Cu(18.1)/P(4)-SiO_2	8.9	2.4	11.6	29.0	14.6	28.2	14.3

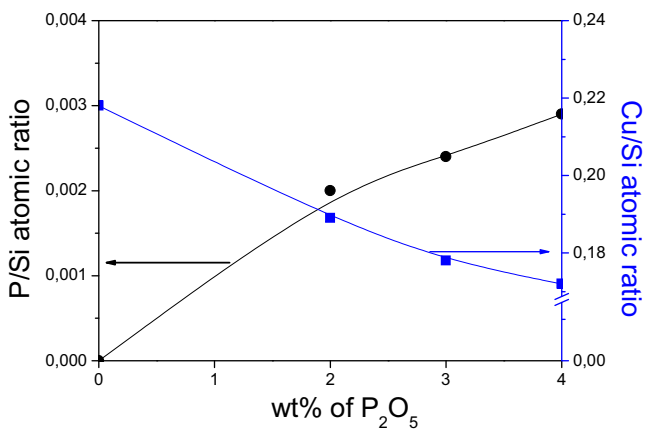

Fig. 6. Calculated and measured XPS P/Si and Cu/Si atomic ratios as a function of P_2O_5 content.

enhanced the activity in the catalytic removal of N and S compounds, and probably O compounds too. Therefore, the distortion of the octahedral geometry of CuO species with P_2O_5 addition (Fig. 4) can lead to higher Cu-Cu metallic distance, similar to that observed for Ni [34], increasing the electron density [35]. This will consequently increase the activity in glycerol conversion. However, the electronic and geometrical effect of P_2O_5 on Cu catalysts favors the catalytic activity only with the lowest P content (2 wt% of P_2O_5), were this effect compensates for the loss of dispersion observed by XPS measurements. For the catalysts with higher P content (3 and 4 wt% of P_2O_5) a more remarkable decrease of Cu dispersion (XPS results) lead to loss of active sites by aggregates formation, leading to decrease in activity despite the presence of Cu-P interaction.

Table 3 presents the products distribution over Cu(18.4)/SiO_2 and Cu(x)/P(y)-SiO_2 catalysts. It shows that before P_2O_5 addition, the principal products were 1.2-PDO and 1-propanol, which are typical products from supported Cu catalysts. However, all the Cu(x)/P(y)-SiO_2 catalysts presented 1-propanol and propanoic acid as principal products of the reaction. According to several proposed reaction schemes [8,16,17], acrolein is formed after two dehydration steps, followed by hydration to propanoic acid. Therefore, the increase of the formation of acrolein and propanoic acid can be attributed to P-OH and Si-OH acid sites formed in the aqueous solution during the reaction [35], which also improved the catalytic activity by Cu stabilization on the surface of the support.

4. Conclusions

The present study showed that the addition of P_2O_5 modified the reactivity of supported Cu catalysts and had a positive effect on the hydrogenolysis activity of glycerol. The addition of P_2O_5 induced changes in the electronic and geometrical properties of Cu(x)/P-SiO_2 catalysts. The Cu-P interactions inferred from TPR measurements were supported by observed distortion of the octahedral symmetry of CuO by the presence of P_2O_5 determined by UV-DRS analyses. This observed interaction led to a decrease of the Cu/Si atomic ratio. The loss of dispersion due to Cu-P interaction was compensated for by an increase of Cu-P electron density only at 2 wt% of P_2O_5 loading, which favors adsorption on the C—O bond of glycerol. For the catalysts with P content above 2 wt%, the formation of aggregates led to loss of active sites and a consequent decrease in activity. In relation to products distribution, the addition of P led to an increase of dehydrated and hydrated compounds such as propanoic acid and acrolein due to P-OH and Si-OH acid sites formed in aqueous solution during the reaction.

Acknowledgments

C. Sepúlveda thanks CONICYT-Chile for FONDECYT N° 11130376, and FONDEQUIP EQM 120096 grants.

References

[1] C.-H. Zhou, J.N. Beltramini, Y.-X. Fan, G.Q. Lu, Chem. Soc. Rev. 37 (2008) 527–549.
[2] G.W. Huber, S. Iborra, A. Corma, Chem. Rev. 106 (2006) 4044–4098.
[3] Y. Gu, J. Barrault, F. Jérôme, Adv. Synth. Catal. 350 (2008) 2007–2012.
[4] S. Gil, M. Marchena, L. Sánchez-Silva, A. Romero, P. Sánchez, J.L. Valverde, Chem. Eng. J. 178 (2011) 423–435.
[5] Y. Kusunoki, T. Miyazawa, K. Kunimori, K. Tomishige, Catal. Commun. 6 (2005) 645–649.
[6] M.S. Khayoon, B.H. Hameed, Appl. Catal. A 433–434 (2012) 152–161.
[7] F.J. Gutiérrez Ortiz, F.J. Campanario, P.G. Aguilera, P. Ollero, Energy 84 (2015) 634–642.
[8] A. Bienholz, H. Hofmann, P. Claus, Appl. Catal. A 391 (2011) 153–157.
[9] S.S. Priya, V.P. Kumar, M.L. Kantam, S.K. Bhargava, S. Periasamy, K.V.R. Chary, Appl. Catal. A 498 (2015) 88–98.
[10] Z. Huang, F. Cui, J. Xue, J. Zuo, J. Chen, C. Xia, Catal. Today 183 (2012) 42–51.
[11] A. Corma, S. Iborra, A. Velty, Chem. Rev. 107 (2007) 2411–2502.
[12] R.M. West, E.L. Kunkes, D.A. Simonetti, J.A. Dumesic, Catal. Today 147 (2009) 115–125.
[13] L. Li, D. Mao, J. Yu, X. Guo, J. Power Sources 279 (2015) 394–404.
[14] E.S. Vasiliadou, T.M. Eggenhuisen, P. Munnik, P.E. de Jongh, K.P. de Jong, A.A. Lemonidou, Appl. Catal. B 145 (2014) 108–119.
[15] R.V. Sharma, P. Kumar, A.K. Dalai, Appl. Catal. A 477 (2014) 147–156.
[16] F. Vila, M. López Granados, M. Ojeda, J.L.G. Fierro, R. Mariscal, Catal. Today 187 (2012) 122–128.
[17] I. Gandarias, P.L. Arias, J. Requies, M.B. Güemez, J.L.G. Fierro, Appl. Catal. B 97 (2010) 248–256.
[18] L. Ma, D. He, Z. Li, Catal. Commun. 9 (2008) 2489–2495.
[19] N. Hamzah, N.M. Nordin, A.H.A. Nadzri, Y.A. Nik, M.B. Kassim, M.A. Yarmo, Appl. Catal. A 419–420 (2012) 133–141.
[20] E.P. Maris, R.J. Davis, J. Catal. 249 (2007) 328–337.
[21] E.S. Vasiliadou, A.A. Lemonidou, Appl. Catal. A 396 (2011) 177–185.
[22] P. Rayo, J. Ramírez, P. Torres-Mancera, G. Marroquín, S.K. Maity, J. Ancheyta, Fuel 100 (2012) 34–42.
[23] K. Leiva, C. Sepúlveda, R. García, J.L.G. Fierro, G. Aguila, P. Baeza, M. Villarroel, N. Escalona, Appl. Catal. A 467 (2013) 568–574.
[24] J. Huang, J. Chen, Chin. J. Catal. 33 (2012) 790–796.
[25] R. Cid, G. Pecchi, Appl. Catal. 14 (1985) 15–21.
[26] K.V.R. Chary, K.K. Seela, G.V. Sagar, B. Sreedhar, J. Phys. Chem. B 108 (2004) 658–663.
[27] A.J. Marchi, J.L.G. Fierro, J. Santamaría, A. Monzón, Appl. Catal. A 142 (1996) 375–386.
[28] L.-F. Chen, P.-J. Guo, M.-H. Qiao, S.-R. Yan, H.-X. Li, W. Shen, H.-L. Xu, K.-N. Fan, J. Catal. 257 (2008) 172–180.
[29] M.L. Smith, A. Campos, J.J. Spivey, Catal. Today 182 (2012) 60–66.
[30] G.V. Mamontov, O.V. Magaev, A.S. Knyazev, O.V. Vodyankina, Catal. Today 203 (2013) 122–126.
[31] R. Hierl, H. Knözinger, H.-P. Urbach, J. Catal. 69 (1981) 475–486.
[32] H. Praliaud, S. Mikhailenko, Z. Chajar, M. Primet, Appl. Catal. B 16 (1998) 359–374.

[33] B.R. Strohmeier, D.E. Levden, R.S. Field, D.M. Hercules, J. Catal. 94 (1985) 514–530.
[34] C. Stinner, Z. Tang, M. Haouas, T. Weber, R. Prins, J. Catal. 208 (2002) 456–466.
[35] Y.-K. Lee, S.T. Oyama, J. Catal. 239 (2006) 376–389.
[36] C.W. Fitz, H.F. Rase, Ind. Eng. Chem. Prod. Rd. 22 (1983) 40–44.
[37] J. Agrell, H. Birgersson, M. Boutonnet, I. Melián-Cabrera, R.M. Navarro, J.L.G. Fierro, J. Catal. 219 (2003) 389–403.
[38] T.A. Zepeda, B. Pawelec, J.L.G. Fierro, A. Montesinos, A. Olivas, S. Fuentes, T. Halachev, Microporous Mesoporous Mat. 111 (2008) 493–506.

Please cite this article in press as: C. Sepúlveda, et al., Effect of phosphorus on the activity of Cu/SiO_2 catalysts in the hydrogenolysis of glycerol, Catal. Today (2016), http://dx.doi.org/10.1016/j.cattod.2016.06.004